Laser speckle contrast imaging: age-related changes in microvascular blood flow and correlation with pulse-wave velocity in healthy subjects

Adil Khalil
Anne Humeau-Heurtier
Guillaume Mahé
Pierre Abraham

SPIE.

Laser speckle contrast imaging: age-related changes in microvascular blood flow and correlation with pulse-wave velocity in healthy subjects

Adil Khalil,[a] Anne Humeau-Heurtier,[a,*] Guillaume Mahé,[b] and Pierre Abraham[c]
[a]University of Angers, LARIS-Laboratoire Angevin de Recherche en Ingénierie des Systémes, 62 Avenue Notre-Dame du Lac, 49000 Angers, France
[b]Pôle Imagerie Médicale et Explorations Fonctionnelles, Inserm CIC 1414, Hospital Pontchaillou of Rennes, University of Rennes 1, 35033 Rennes Cedex 9, France
[c]University of Angers, Hospital of Angers, Laboratoire de Physiologie et d'Explorations Vasculaires UMR CNRS 6214-INSERM 1083, 49033 Angers Cedex 01, France

Abstract. In the cardiovascular system, the macrocirculation and microcirculation—two subsystems—can be affected by aging. Laser speckle contrast imaging (LSCI) is an emerging noninvasive optical technique that allows the monitoring of microvascular function and can help, using specific data processing, to understand the relationship between the subsystems. Using LSCI, the goals of this study are: (i) to assess the aging effect over microvascular parameters (perfusion and moving blood cells velocity, MBCV) and macrocirculation parameters (pulse-wave velocity, PWV) and (ii) to study the relationship between these parameters. In 16 healthy subjects (20 to 62 years old), perfusion and MBCV computed from LSCI are studied in three physiological states: rest, vascular occlusion, and post-occlusive reactive hyperaemia (PORH). MBCV is computed from a model of velocity distribution. During PORH, the experimental results show a relationship between perfusion and age ($R^2 = 0.67$) and between MBCV and age ($R^2 = 0.72$), as well as between PWV and age at rest ($R^2 = 0.91$). A relationship is also found between perfusion and MBCV for all physiological states ($R^2 = 0.98$). Relationships between microcirculation and macrocirculation (perfusion-PWV or MBCV-PWV) are found only during PORH with $R^2 = 0.76$ and $R^2 = 0.77$, respectively. This approach may prove useful for investigating dysregulation in blood flow. © 2015 Society of Photo-Optical Instrumentation Engineers (SPIE) [DOI: 10.1117/1.JBO.20.5.051010]

Keywords: laser speckle contrast imaging; biomedical optics; image processing; blood flow; Lorentzian profile.

Paper 140535SSRR received Aug. 25, 2014; accepted for publication Oct. 29, 2014; published online Nov. 25, 2014.

1 Introduction

The arterial network of the cardiovascular system (CVS) is composed of two subsystems, macro- and microcirculation, which interact to enable an optimal adaptation to various physiologic disturbances. With age and/or risk factors such as hypertension and pathologies such as diabetes, modifications appear in both the macro- and microcirculation subsystems (see, e.g., Refs. 1 and 2). The monitoring and analyses of large vessels' characteristics (such as the arteries) provide a good vital biomarker to assess the status of macrocirculation. Thus, pulse-wave velocity (PWV) is a measure of arterial stiffness. The latter is considered an important predictor of cardiovascular events.[3–5] On the other hand, assessment of microvascular blood flow has been recognized as important for the follow-up of pathologies such as diabetes or Raynaud's phenomenon but also to analyze the effects of aging.[6,7] Thus, it has been shown that age changes the morphology and quantification of the cutaneous microvasculature.[6,8] Moreover, age is a primary risk factor for cardiovascular disease.[9]

Different optical techniques have emerged to monitor microvascular blood flow.[10–13] Laser speckle contrast imaging (LSCI) has the advantage of being noninvasive, contactless, highly reproducible, leading to high temporal and spatial resolution images of the microvascular blood perfusion, and requiring low-cost devices.[14–16] Moreover, when assumptions are made on the moving scatterers' velocity profile, LSCI data provide information on red blood cells' velocity values.[17]

Studying the relationship between macro- and microcirculation may lead to an early estimation of many disorders in the CVS. Several authors emphasized that the two subsystems, macrocirculation and microcirculation, must be simultaneously taken into account.[1,18]

In this work, we propose to analyze the impact of age on data recorded simultaneously from the macrocirculation (PWV) and the microcirculation (LSCI) in healthy subjects. The analysis in healthy subjects is important as it is the first step before an analysis in pathological subjects. Our goals are, therefore, the following: study the evolution with age of (1) the possible correlation between PWV and LSCI microvascular perfusion; (2) the possible correlation between PWV and microvascular red blood cells' velocity extracted from LSCI data; and (3) the possible correlation between microvascular perfusion and microvascular red blood cells' velocity extracted from LSCI data. Furthermore, for the three above mentioned items, three physiological states are analyzed: rest, vascular occlusion, and post-occlusive hyperaemia peak.

In what follows, we first present the LSCI theoretical background and the way to estimate moving blood cells' velocity

*Address all correspondence to: Anne Humeau-Heurtier, E-mail: anne .humeau@univ-angers.fr

from LSCI data. Then the measurement procedure used to acquire data from the macro- and the microcirculation subsystems is described. The processing algorithm used to process PWV and LSCI data is then detailed. Finally, we present our findings and discuss them.

2 Materials and Methods

2.1 Laser Speckle Contrast Imaging

2.1.1 LSCI Principles

LSCI relies on a laser source and a camera. When a laser source diffuses a light over the desired area of tissue, the photons of the laser light are backscattered by both moving (such as red blood cells) and static (such as skin) scatterers. The backscattered light forms an interference pattern of bright and dark pixels, called speckle, on the camera. The movements in the illuminated sample (i.e., movements of blood cells) lead to temporal changes in the speckle pattern. Due to the exposure time T of the camera, a blurring in the speckle pattern is obtained. To quantify the degree of blurring, the spatial contrast K is used and computed as[17]

$$K = \frac{\sigma_s}{\langle I \rangle}, \tag{1}$$

where σ_s refers to the spatial standard deviation in a small region around a pixel of the speckle raw data, whereas $\langle I \rangle$ is the mean intensity around that pixel. A speckle contrast K close to 1 indicates that there is no blurring of the speckle pattern and, therefore, no motion. Alternatively, K values closer to 0 mean that the scatterers are moving fast enough to blur all the speckles.

The value of speckle contrast K can be obtained directly by computing Eq. (1) from the pixels in a surrounding $N \times N$ window. The size of the window at which the speckle contrast is computed is critical:[19] the statistics are compromised with too few pixels. By opposition, the spatial resolution is sacrificed with too many pixels. It has been reported that a square window of size 5×5 pixels^2 or 7×7 pixels^2 would be convenient.[19] To obtain a two-dimensional contrast image reflecting the local motion due to blood flow, a sliding window is used to move along the raw speckle image. Perfusion is then computed from the inverse of the contrast value (see an example of a perfusion image in Fig. 1).

From contrast K values, moving blood cells' velocity values can be extracted provided assumptions are made on the velocity profile of the moving scatterers. This is due to the fact that the variance $\sigma_s^2(T)$ of the spatial intensity distribution in a time-averaged speckle pattern with an integration time T is linked to the autocovariance $C_t(\tau)$ of the temporal fluctuations in the intensity fluctuations of a single speckle:[20]

$$\sigma_s^2(T) = \frac{2}{T} \int_0^T \left(1 - \frac{\tau}{T}\right) C_t(\tau) d\tau, \tag{2}$$

where $C_t(\tau)$ depends, among others, on the velocity distribution of the scattering particles.[20,21]

The choice of velocity profile has a major effect on the relation between the speckle contrast K and velocity values.[22,23] Thus, it has been shown that the relation between speckle contrast K and the ratio τ_c/T (where τ_c is the correlation time of the intensity fluctuations) is critically related to the velocity distribution.[23] Several authors used the Lorentzian model to link the motion of the scatterers and the speckle contrast K.[17,20,24] This is appropriate for a Brownian motion (unordered flow).

2.1.2 Computation of Moving Blood Cells Velocity from LSCI Data

The autocovariance $C_t(\tau)$ of the temporal fluctuations in the intensity fluctuations of a single speckle is defined as

$$C_t(\tau) = \langle [I(t) - \langle I \rangle_t][I(t + \tau) - \langle I \rangle_t] \rangle_t, \tag{3}$$

where $\langle \rangle_t$ indicates a time-averaged quantity. We also have

$$g_2(\tau) = 1 + \frac{C_t(\tau)}{\langle I \rangle_t^2}, \tag{4}$$

where $g_2(\tau)$ is the intensity temporal autocorrelation function. We can also write (Siegert relation):

$$g_2(\tau) = 1 + \beta |g_1(\tau)|^2, \tag{5}$$

where $g_1(\tau)$ is the electric field temporal autocorrelation function and β accounts for the loss of correlation related to the ratio of the detector (or pixel) size to the speckle size and to polarization. From Eqs. (2), (4), and (5), and assuming ergodicity[20] (we can, in this case, replace the time average by the ensemble average), we have to solve the equation
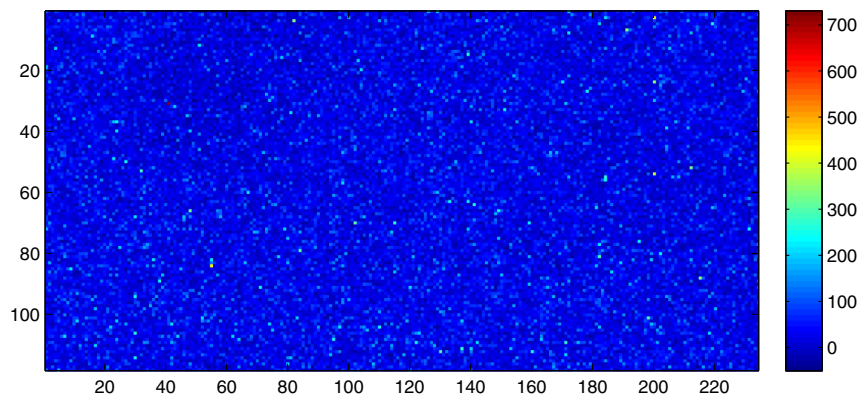

Fig. 1 Experimental perfusion image (118×234 pixels^2) of forearm in a healthy subject obtained with LSCI technique.

$$K^2 = \frac{2\beta}{T} \int_0^T \left(1 - \frac{\tau}{T}\right) |g_1(\tau)|^2 d\tau, \tag{6}$$

to obtain an analytical expression of the contrast K for the velocity distributions mentioned above.

The Lorentzian profile is the most commonly used profile to determine the theoretical expression of contrast K.[17,20,22,24,25] If the moving scatterers are assumed to follow a Lorentzian distribution, we have (see, e.g., Ref. 25)

$$g_1(\tau) = \exp\left(-\frac{|\tau|}{\tau_c}\right), \tag{7}$$

where τ_c is the correlation time of the intensity fluctuations. Solving Eq. (6), the contrast K for a Lorentzian distribution can be written as

$$K_{\text{Lorentzien}} = \beta^{1/2} \left\{ \frac{1}{x} + \frac{1}{x^2} [\exp(-2x) - 1] \right\}^{1/2}, \tag{8}$$

where $x = T/\tau_c$.

The relationship between correlation time τ_c and moving blood cells in the microcirculation is assumed to be an inverse one. Therefore, from the experimental values of contrast K, the velocity of moving scattering particles can be calculated as[17]

$$v_c = \frac{\lambda}{2\pi\tau_c}, \tag{9}$$

where λ is the laser wavelength.

2.1.3 Effect of Static Scattering

The expression of speckle contrast K is used to determine the velocity of the moving blood cells in the microcirculation. Nevertheless, Eq. (8) does not take into account the presence of static scatterers (such as bones, skin, and skull). It has been reported that if the static scatterers effect is not considered, then it results in an underestimation of the spatial and temporal variations in the sample dynamics.[8,26] Moreover, some authors mentioned that the computation of blood flow velocity from LSCI data leads to erroneous values when the presence of static scatterers is not taken into account.[27] Only a few authors studied the effect of static scatterers on the estimation of moving blood cells velocity from the expression of speckle contrast K (see, e.g., Ref. 28).

By assuming a Lorentzian velocity profile for the moving scatterers, and when static scatterers are taken into account, the expression of speckle contrast K becomes[28]

$$\begin{aligned} K_{\text{Lorentzien}} = \beta^{1/2} &\left[\rho^2 \frac{\exp(-2x) - 1 + 2x}{2x^2} \right. \\ &\left. + 4\rho(1 - \rho) \frac{\exp(-x) - 1 + x}{x^2} + (1 - \rho)^2 \right]^{1/2} \\ &+ C_{\text{noise}}, \end{aligned} \tag{10}$$

where $x = T/\tau_c$, $\rho = I_f/(I_f + I_s)$ with I_f the time-averaged intensity of the fluctuating dynamically scattered light, I_s the intensity of the statically scattered light, and C_{noise} a measurement noise such as shot noise or camera readout noise.[28] From

this latter expression and using Eq. (9), moving blood cells' velocity can be computed when static scatterers are considered. Moreover, in the laser speckle contrast imager used for the experimental acquisition (see below), we have (from Perimed documentation)

$$\text{Perfusion} \sim \frac{1}{K} - 1. \tag{11}$$

Using Eqs. (9) and (10), we thus obtain the relation linking the perfusion and the velocity of moving scattering particles

$$\begin{aligned} \text{Perfusion} \sim &\left\{ \beta^{1/2} \left[\rho^2 \frac{\exp(-4\alpha v_c) - 1 + 4\alpha v_c}{8(\alpha v_c)^2} \right. \right. \\ &\left. + 4\rho(1 - \rho) \frac{\exp(-2\alpha v_c) - 1 + 2\alpha v_c}{4(\alpha v_c)^2} + (1 - \rho)^2 \right]^{1/2} \\ &\left. + C_{\text{noise}} \right\}^{-1} - 1, \end{aligned} \tag{12}$$

where $\alpha = \pi T/\lambda$.

In order to obtain an experimental ρ value, the following expression was used[29]

$$\rho = 1 - \beta^{-1/2} \left[\frac{\langle I_1 I_2 \rangle}{\langle I_1 \rangle \langle I_2 \rangle} - 1 \right]^{1/2}, \tag{13}$$

where I_1 and I_2 are two sequential intensity images, $\langle I \rangle$ denotes the spatial averaging of the intensity over a selected area containing N pixels, and $\langle I_1 I_2 \rangle = (1/N) \sum_{i=1}^N I_1(x_i) I_2(x_i)$.

2.2 Subjects Preparation

In this study, 16 healthy subjects without known disease have been studied. These 16 subjects have been subdivided into two groups. The first group included eight young subjects (three women and five men, body mass index $= 22.57 \pm 2.88$ kg/m^2, resting blood pressure: systolic $= 114.8 \pm 11.2$ mm Hg, diastolic $= 66.4 \pm 6.4$ mmHg) who were younger than 30 years old (aged between 20 and 30 years). The second group included eight elderly subjects (eight women, body mass index $= 22.68 \pm 1.61$ kg/m^2, resting blood pressure: systolic $= 116.1 \pm 7.3$ mm Hg, diastolic $= 71.3 \pm 8.5$ mm Hg) who were older than 50 years old (aged between 50 and 62 years). All the subjects provided written, informed consent prior to participation and the study was carried out in accordance with the declaration of Helsinki. For the data recordings, subjects were supine in a quiet room with a controlled temperature[30] and without any air movement.[31]

2.3 Experimental Set-up

For the recordings of the PWV signals, a Mobil-O-Graph (ambulatory blood pressure and 24-h PWA monitor, Germany) was used. The PWV was recorded for each subject, at rest, at the forearm level.

For the recordings of LSCI data, a PeriCam PSI System (Perimed, Sweden) having a laser wavelength of 785 nm and an exposure time T of 6 ms was used and the superficial blood flow from the ventral face of the forearm was recorded

in laser speckle perfusion units (LSPU). The sampling frequency for the acquisitions was 16 Hz. Moreover, the distance between the laser head to forearm skin was adjusted to 15 ± 1 cm[32] which gave images with a resolution around 0.45 mm. Contrast images were stored on a computer for off-line analysis. For LSCI data, the recording procedure was composed of three physiological states: (1) 2 min at rest (period during which PWV was recorded), (2) 3 min of vascular occlusive (biological zero),[33,34] obtained by inflating an arm cuff to 220 mmHg, and (3) 5 min of post-occlusive reactive hyperaemia.

2.4 Image and Signal Processing Procedure

In our work, two cases have been studied: (1) $\rho = 1$, which corresponds to the case where static scatterers are not taken into account; (2) $\rho \neq 1$, the ρ value for each subject was determined from Eq. (13). Afterward, Eq. (10) led to the determination of the moving blood cells' velocity values for the two cases. The following image processing procedure was used:

1. On the first image of each image sequence, a pixel was chosen randomly and its contrast value was followed in time.

2. A ROI of 5×5 pixels^2 has been determined around the pixels mentioned in step (1). The mean of the contrast values inside each ROI was computed. This operation has been carried out over all the images in the image sequence to obtain contrast time evolution signals.

3. LSCI data are, by definition, very sensitive to movements.[35,36] These artefacts appear as high and transient peaks in the data. To remove movement artifacts and get a reasonable LSCI signal, each contrast time evolution signal was passed through a low-pass sixth order Butterworth digital filter with a cutoff frequency of 3 Hz (see, e.g., Ref. [37]).

4. From Eq. (10), we determined the value of the speckle correlation time τ_c for each image of the image sequence. For the numerical determination of the correlation time τ_c from contrast values K, we used a combination of bisection, secant, and an inverse quadratic interpolation method.[38,39] From the values of τ_c, the velocity of the red blood cells has then been determined from Eq. (9). This has been performed for each subject in the two cases: $\rho = 1$ and ρ computed from Eq. (13).

2.5 Statistical Analysis

Statistical analyses were performed using MedCalc for Windows, version 12.5 (MedCalc Software, Ostend, Belgium). Using the Wilcoxon test, we compared velocity values obtained for young subjects with the ones obtained for the elderly subjects. For each statistical analysis, a P value < 0.05 was considered significant.

3 Results and Discussion

When using Eq. (13), the values of ρ obtained for each population are mentioned in Table 1. We observe that the average

Table 1 Average values of ρ computed from Eq. (13) in two groups (young and elderly) of eight subjects each (see text for details).

Young	Elderly
0.94 ± 0.04	0.94 ± 0.06

value of ρ for the younger group does not differ significantly from the one obtained with the elderly subjects. With these ρ values and during post-occlusive reactive hyperaemia, we observe a strong correlation between perfusion and age and between velocity and age, as well as between PWV and age at rest (R^2 equal to 0.67, 0.63, 0.91, respectively). For $\rho = 1$ in the computation of the velocity values, we also obtain a strong correlation between velocity and age (R^2 equal to 0.72). Our first findings are, therefore, that the studied parameters of microcirculation and macrocirculation are correlated with age.

Moreover, Fig. 2 shows the evolution of microvascular blood cells' velocity with perfusion for the three physiological states (rest, vascular occlusion, and post-occlusive reactive hyperaemia), and for all the subjects when the static scatterers effect is neglected ($\rho = 1$). From this figure, we observe that moving blood cell velocity values increase with perfusion values. We also note a strong correlation between them (Velocity $= 0.21 \times$ Perfusion$^{1.27}$, $R^2 = 0.98$). Moreover, we note that the highest moving blood cell velocity values (and, therefore, the highest perfusion values) are obtained for the aged subjects during post-occlusive reactive hyperaemia. When $\rho = 1$, strong correlations are also obtained between perfusion values obtained during post-occlusive reactive hyperaemia and PWV values (see Fig. 3), as well as between moving blood cell velocity obtained during post-occlusive reactive hyperaemia and PWV values (see Fig. 4): for perfusion values recorded during post-occlusive reactive hyperaemia and PWV,
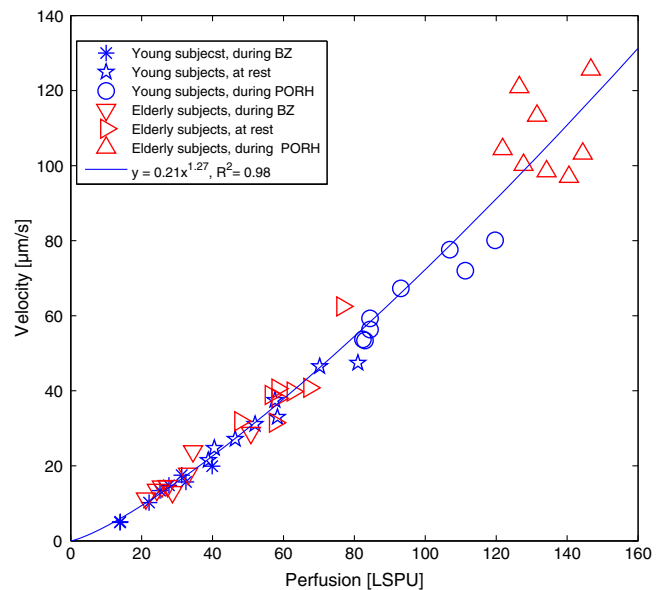

Fig. 2 Moving blood cells' velocity values and perfusion values computed from LSCI data for 16 subjects, at rest, during vascular occlusion and post-occlusive reactive hyperaemia (see text for details). Curve shows line of best fit by least squares. The value of ρ has been set to 1.
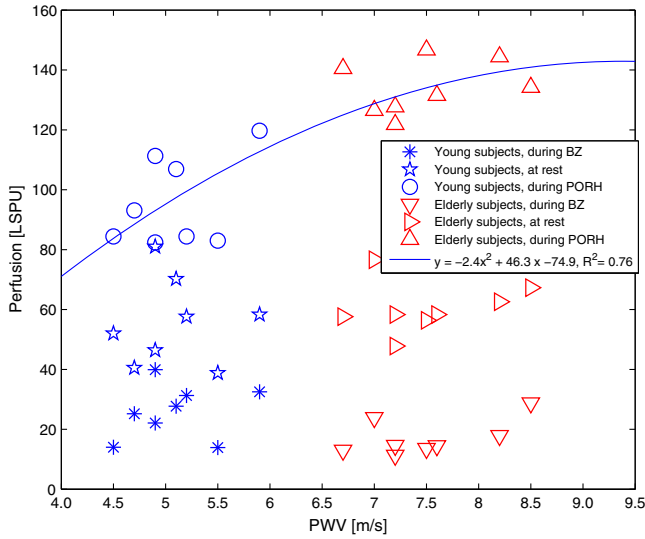
Fig. 3 LSCI perfusion values, at rest, during vascular occlusion and post-occlusive reactive hyperaemia and PWV values, for 16 subjects (see text for details). Curve shows line of best fit by least squares for data recorded during post-occlusive reactive hyperaemia.

we have Perfusion $= -2.4 \times \mathrm{PWV}^2 + 46.3 \times \mathrm{PWV} - 74.9$, $R^2 = 0.76$; for moving blood cells' velocity recorded during post-occlusive reactive hyperaemia and PWV, we have Velocity $= -4.4 \times \mathrm{PWV}^2 + 72.3 \times \mathrm{PWV} - 184.7$, $R^2 = 0.77$. For the other physiological states (rest and biological zero), the correlation is much lower ($R^2 < 0.3$).

In this study, we also studied the effect of static scatterers on velocity values of moving blood cells computed from LSCI data. The mean velocity values obtained with the ρ values computed from Eq. (13) for each subject are mentioned in Table 2. Our results show that static scatterers have an effect on the velocity values of moving scatterers computed from LSCI data, at rest, during vascular occlusion and during post-occlusive reactive hyperaemia: velocity values of moving scatterers
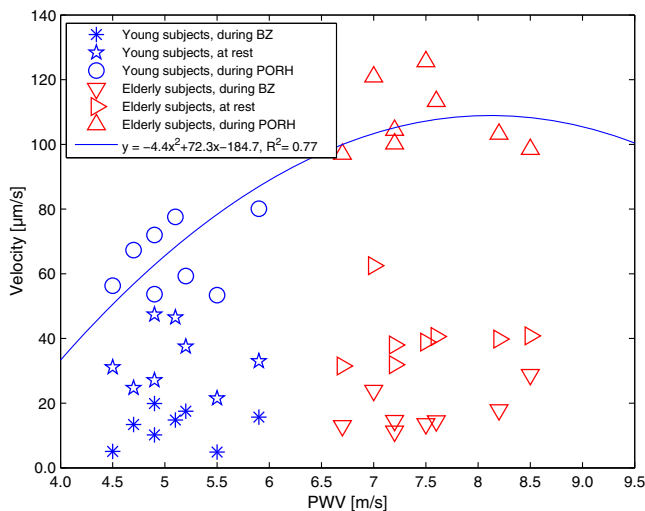

Fig. 4 Moving blood cells' velocity values computed from LSCI data, at rest, during vascular occlusion and post-occlusive reactive hyperaemia and PWV values, for 16 subjects (see text for details). Curve shows line of best fit by least squares for data recorded during post-occlusive reactive hyperaemia. The value of ρ has been set to 1.

Table 2 Mean velocity results (μm/s) of moving scatterers computed from LSCI data. Three physiological states are analyzed: 1 min at rest, 1 min during biological zero and 3 s during post-occlusive reactive hyperaemia peak. The results are obtained from two groups (young and elderly) of eight subjects each when a Lorentzian velocity profile is assumed for moving scatterers.

ρ	$\rho = 1$		ρ computed from Eq. (13)	
Group	Young	Elderly	Young	Elderly
Rest	34.5	40.5	40.0	45.8
Biological zero	13.0	15.6	14.0	18.8
Hyperaemia	66.6*	109.3	77.1*	130.4

Note: * means statistically significant with results obtained from the elderly group. The results are obtained from ROI of 5×5 pixels^2. Two cases are presented: $\rho = 1$ which corresponds to the case where static scatterers are not taken into account and $\rho \neq 1$ [ρ computed from Eq. (13)] where the static scatterers' effect is considered.

increase when the static scatterers' effect is taken into account (in this case $\rho < 1$). Furthermore, we can observe that at rest and during vascular occlusion, the mean velocities' values found for young subjects are lower than the ones obtained for elderly subjects. This is true when the static scatterers effect is taken into account and when it is not. Nevertheless, these differences are not statistically significant. From the literature, the value of basal blood flow (product of velocity by concentration of moving blood cells) for young and elderly subjects remains debatable (see, e.g., Refs. 40 and 41). Alternatively, during post-occlusive reactive hyperaemia, there is an obvious difference in the mean velocity values between young and elderly people (see Table 2). Thus, the mean velocities obtained from the elderly group are statistically higher than the ones obtained from the young people. This is true when the static scatterers' effect is taken into account and when it is not. This may be due to the stiffness of vessels that increases with age. PWV is a measure of arterial stiffness[42] and it is recognized that it increases with age. Our results regarding PWV are, therefore, in accordance with what was expected. Because stiffness is higher for aged people, the revascularization of vessels after the vascular occlusion (post-occlusive reactive hyperaemia) may lead to higher moving blood cells' velocity values.

The effect of static scatterers on the correlation R^2 values between moving scatterers' velocity and PWV is shown in Table 3. From this table, we observe that the correlation values do not vary much in the presence or absence of static scatterers.

Table 3 Correlation values computed between velocity and PWV when LSCI data are recorded at rest, during biological zero (BZ) and during a post-occlusive reactive hyperaemia (PORH). PWV is recorded at rest. See text for details.

ρ	$\rho = 1$			ρ computed from Eq. (13)		
Biological state	Rest	BZ	PORH	Rest	BZ	PORH
Correlation between velocity and PWV	0.13	0.29	0.77	0.11	0.32	0.71

To the best of our knowledge, no other group has worked on the impact of aging on moving blood cells' velocity computed from LSCI data. Moreover, our work is the first one to simultaneously assess LSCI perfusion, moving blood cells' velocity and PWV. This analysis has been performed on two populations: a younger and an older one. Skin aging has been thoroughly studied and is still the subject of many works (see, e.g., Ref. [43]).

Age-related changes play an important role in the pathogenesis of many diseases.[44–47] Previous studies in elderly subjects suggested impairments of microvascular reactivity upon aging.[48,49] With aging, a number of hypoxia- and metabolism-related changes occur.[40,50,51] These changes are due to alterations in the microcirculation. Moreover, as mentioned recently,[48] the number of functioning capillaries diminishes with age, and phenomena such as vascular rarefaction, appearance of zones of complete vascular obliteration, irregular caliber of microvessels,[52–54] and inhibition of the processes of angiogenesis[55] may appear. As pointed out by Gates et al.,[56] capillary rarefaction may be due to vessel destruction, impaired angiogenesis, and impaired vasculogenesis. Oxidant stress may also contribute to capillary rarefaction by inducing endothelial cell apoptosis and/or reducing the nitric oxide needed for vascular budding and stimulation of vascular endothelial growth factor. Aging is accompanied by suppression of the endothelial function and cellular metabolism, degeneration of the sensor and sympathetic innervation.[57,58] Moreover, it has been reported that aging may involve alterations in nitric oxide, prostanoid, endothelium-derived hyperpolarizing factor(s), and endothelin-1 pathways.[56] Aging also leads to a degradation of a number of extracellular matrix proteins, including collagen and elastic fibers.[59,60] The study of post-occlusive hyperaemia is, therefore, of importance as it is mediated by two major mediators: sensory nerves and endothelium-derived hyperpolarizing factors. Furthermore, we have to note that skin thickness could vary with age.[61] Thus, the stratum corneum is generally accepted to maintain its thickness during aging. However, dermal, epidermal, and whole skin thickness changes are controversial. Ultrasound reveals the appearance of a subepidermal low echogenic band that thickens with age (due to changes in collagen structure), especially in environmentally exposed areas.[61] Some studies also indicate the presence of an echogenic band in the lower dermis which thins with increased age. However, the whole dermis appears to become more echogenic in elderly people.[61]

Studies have reported an attenuated vasodilator response of skin microcirculation to a variety of stimuli with age.[62–65] This attenuation is thought to be the result of endothelial dysfunction.[56] Thus, Tikhonova et al. recently reported a higher increase of perfusion in young people compared to aged subjects after an occlusion removal.[48] Hagisawa et al. reported the same conclusion some years before.[62] These findings are different from ours: during post-occlusive reactive hyperaemia, we found the highest perfusion values for the aged subjects. The discrepancy may be explained by differences in at least three parameters: (1) to monitor microvascular blood flow Tikhonova et al., as well as Hagisawa et al., employed a different technique from the one used in our work: they used laser Doppler flowmetry while we used LSCI. These two techniques do not probe the same volume of tissue (laser Doppler flowmetry probes deeper than LSCI);[66] (2) the age ranges studied are different: Tikhonova et al. studied a group composed of people between 19 and 30 years old and another group composed of people between 30

and 60 years old.[48] Hagisawa et al. studied a group composed of people between 22 and 27 years old and another group composed of people between 62 and 68 years old.[62] In our younger group, people were between 20 and 30 years old, whereas in our older group, people were between 50 and 62 years old; and (3) the effect of fitness. It has been reported that effect of fitness has an influence on the peak of post-occlusive reactive hyperaemia: Tew et al. found a higher post-occlusive reactive hyperaemia peak in aged fit participants than in active young subjects, and the post-occlusive reactive hyperaemia peak in active subjects was higher than for sedentary aged subjects.[41] The latter study was conducted through laser Doppler flowmetry signals. Moreover, microvessel function is worse in older sedentary compared with older active or younger men, and this is attributable to impaired nitric oxide signalling.[67] Other factors may also explain the differences between our results and the ones of Tikhonova et al., as medical drugs (e.g., at age-specific and hormone replacement therapy) and other vasoactive substances. Furthermore, it has previously been reported that gender has an impact on microcirculation,[68] which was not studied in our work.

In our analysis, three physiological states have been studied: rest, vascular occlusion, and post-occlusive reactive hyperaemia. The biological zero has been the subject of many studies (see, e.g., Refs. [69] and [70]). However, its origin is still not completely known: it is thought to be generated by Brownian motion of the macromolecules within the interstitium[71] or other phenomena related to the function of the autonomic nervous system.[72] Nevertheless, as recently pointed out,[34] this definition may require clarification.

4 Conclusion

This study demonstrates that, in healthy subjects, perfusion and moving blood cells' velocity, two correlated and age-related parameters of microcirculation, are correlated with PWV, a marker of arterial stiffness at the macrovascular level. Future works should be performed in diseased patients. It might be of interest to study these relationships to show whether or not these correlations still exist to try to define new criteria for different diseased states. The latter could lead to modifications in patients' treatment. For example, it has been shown in diabetic patients that PWV is predictive of cardiovascular mortality.[73] It could be of interest to study whether microcirculation parameters can also predict this risk and to assess the time-course of the modifications of microcirculation parameters. Do these modifications appear earlier than PWV modifications? Do microcirculation markers (perfusion or moving blood cells' velocity or both) assessed by optical laser devices predict better the cardiovascular mortality? Do clinicians have an interest in performing both methods to characterize patients' risk?

References

1. F. Feihl, L. Liaudet, and B. Waeber, "The macrocirculation and microcirculation of hypertension," *Curr. Hypertens. Rep.* **11**(3), 182–189 (2009).
2. C. M. Akbari et al., "Endothelium-dependent vasodilatation is impaired in both microcirculation and macrocirculation during acute hyperglycemia," *J. Vasc. Surg.* **28**(4), 687–94 (1998).
3. J. Blacher et al., "Aortic pulse wave velocity as a marker of cardiovascular risk in hypertensive patients," *Hypertension* **33**(5), 1111–1117 (1999).

4. S. Meaume et al., "Aortic pulse wave velocity predicts cardiovascular mortality in subjects >70 years of age," *Arterioscler. Thromb. Vasc. Biol.* **21**(12), 2046–2050 (2001).

5. T. Pereira et al., "Aortic pulse wave velocity and HeartSCORE: improving cardiovascular risk stratification. A sub-analysis of the EDIVA (Estudo de DIstensibilidade VAscular) project," *Blood Pressure* **23**(2), 109–115 (2014).

6. L. Li et al., "Age-related changes of the cutaneous microcirculation in vivo," *Gerontology* **52**(3), 142–153 (2006).

7. S. Tsuda et al., "Pulse-waveform analysis of normal population using laser speckle flowgraphy," *Curr. Eye Res.* [Epub ahead of print] (2014).

8. L. Li et al., "Age-related changes in skin topography and microcirculation," *Arch. Dermatol. Res.* **297**(9), 412–416 (2006).

9. S. S. Najjar, A. Scuteri, and E. G. Lakatta, "Arterial aging is it an immutable cardiovascular risk factor?," *Hypertension* **46**(3), 454–462 (2005).

10. T. J. H. Essex and P. O. Byrne, "A laser Doppler scanner for imaging blood flow in skin," *J. Biomed. Eng.* **13**(3), 189–194 (1991).

11. J. D. Briers, "Laser Doppler, speckle and related techniques for blood perfusion mapping and imaging," *Physiol. Meas.* **22**(4), R35–R36 (2001).

12. A. Humeau-Heurtier et al., "Relevance of laser Doppler and laser speckle techniques for assessing vascular function: state of the art and future trends," *IEEE Trans. Biomed. Eng.* **60**(3), 659–666 (2013).

13. G. Mahe et al., "Impact of experimental conditions on noncontact laser recordings in microvascular studies," *Microcirculation* **19**(8), 669–675 (2012).

14. L. M. Richards et al., "Low-cost laser speckle contrast imaging of blood flow using a webcam," *Biomed. Opt. Express* **4**(10), 2269–2283 (2013).

15. A. Humeau-Heurtier et al., "Excellent inter-and intra-observer reproducibility of microvascular tests using laser speckle contrast imaging," *Clin. Hemorheol. Micro.* [Epub ahead of print] (2013).

16. C. Puissant et al., "Reproducibility of non-invasive assessment of skin endothelial function using laser Doppler flowmetry and laser speckle contrast imaging," *PLoS One* **8**(4), e61320 (2013).

17. J. D. Briers and S. Webster, "Laser speckle contrast analysis (LASCA): a nonscanning, full-field technique for monitoring capillary," *J. Biomed. Opt.* **1**(2), 174–179 (1996).

18. H. A. J. Struijker-Boudier, "The burden of vascular disease in diabetes and hypertension: from micro to macrovascular disease the bad loop," *Medicographia* **31**(3), 251–256 (2009).

19. J. D. Briers, "Laser speckle contrast imaging for measuring blood flow," *Optica Applicata* **37**(1/2), 139–152 (2007).

20. A. F. Fercher and J. D. Briers, "Flow visualization by means of single exposure speckle photography," *Opt. Commun.* **37**(5), 326–330 (1981).

21. J. W. Goodman, *Statistical Optics*, Wiley & Sons, New York (1985).

22. J. C. Ramirez-San-Juan et al., "Impact of velocity distribution assumption on simplified laser speckle imaging equation," *Opt. Express* **16**(5), 3197–3203 (2008).

23. D. Briers et al., "Laser speckle contrast imaging: theoretical and practical limitations," *J. Biomed. Opt.* **18**(6), 066018 (2013).

24. D. D. Duncan and S. J. Kirkpatrick, "Can laser speckle flowmetry be made a quantitative tool?," *J. Opt. Soc. Am. A* **25**(8), 2088–2094 (2008).

25. D. D. Duncan, S. J. Kirkpatrick, and J. C. Gladish, "What is the proper statistical model for laser speckle flowmetry?," *Proc. SPIE* **6855**, 685502 (2008).

26. A. B. Parthasarathy et al., "Robust flow measurement with multi-exposure speckle imaging," *Opt. Express* **16**(3), 1975–1989 (2008).

27. P. Zakharov et al., "Quantitative modeling of laser speckle imaging," *Opt. Lett.* **31**(23), 3465–3467 (2006).

28. D. A. Boas and A. K. Dunn, "Laser speckle contrast imaging in biomedical optics," *J. Biomed. Opt.* **15**(1), 011109 (2010).

29. P. Zakharov et al., "Dynamic laser speckle imaging of cerebral blood flow," *Opt. Express* **17**, 13904–13917 (2009).

30. P. Abraham et al., "Effect of skin temperature on skin endothelial function assessment," *Microvasc. Res.* **88**, 56–60 (2013).

31. G. Mahé et al., "Air movements interfere with laser speckle contrast imaging recordings," *Lasers Med. Sci.* **27**(5), 1073–1076 (2012).

32. G. Mahé et al., "Distance between laser head and skin does not influence skin blood flow values recorded by laser speckle imaging," *Microvasc. Res.* **82**(3), 439–442 (2011).

33. G. B. Tee et al., "Dependence of human forearm skin postocclusive reactive hyperemia on occlusion time," *J. Pharmacol. Toxicol. Methods* **50**(1), 73–78 (2004).

34. I. V. Meglinski et al., "Towards the nature of biological zero in the dynamic light scattering diagnostic modalities," *Doklady Phys.* **58**(8), 323–326 (2013).

35. G. Mahe et al., "Cutaneous microvascular functional assessment during exercise: a novel approach using laser speckle contrast imaging," *Pflugers Arch.* **465**(4), 451–458 (2013).

36. G. Mahé et al., "Laser speckle contrast imaging accurately measures blood flow over moving skin surfaces," *Microvasc. Res.* **81**(2), 183–188 (2011).

37. S. Bricq et al., "Assessing spatial resolution versus sensitivity from laser speckle contrast imaging: application to frequency analysis.," *Med. Biol. Eng. Comput.* **50**(10), 1017–1023 (2012).

38. R. Brent, *Algorithms for Minimization without Derivatives*, Prentice-Hall, Englewood Cliffs, New Jersey (1973).

39. G. E. Forsythe and M. A. Malcolm, and C. B. Moler, *Computer Methods for Mathematical Computations*, Prentice-Hall, Englewood Cliffs, New Jersey (1977).

40. R. Ogrin, P. Darzins, and Z. Khalil, "Age-related changes in microvascular blood flow and transcutaneous oxygen tension under basal and stimulated conditions," *J. Gerontol. Ser. A-Biol. Sci. Med. Sci.* **60**(2), 200–206 (2005).

41. G. A. Tew, M. Klonizakis, and J. M. Saxton, "Effects of ageing and fitness on skin-microvessel vasodilator function in humans," *Eur. J. Appl. Physiol.* **109**(2), 173–181 (2010).

42. I. B. Wilkinson, J. R. Cockcroft, and D. J. Webb, "Pulse wave analysis and arterial stiffness," *J. Cardiovasc. Pharmacol.* **32**(Suppl 3), S33–S37 (1998).

43. J. Vionnet et al., "No major impact of skin aging on the response of skin blood flow to a submaximal local thermal stimulus," *Microcirculation* **21**(8), 730–737 (2014).

44. R. S. Ajmani and J. M. Rifkind, "Hemorheological changes during human aging," *Gerontology* **44**(2), 111–120 (1998).

45. T. F. Lüscher and G. Noll, "Endothelial function as an end-point in interventional trials: concepts, methods and current data," *J. Hypertens. Suppl.* **14**, S111–S121 (1996).

46. E. Makrantonaki and C. C. Zouboulis, "Characteristics and pathomechanisms of endogenously aged skin," *Dermatology* **214**(4), 352–360 (2007).

47. H. Tanaka et al., "Aging, habitual exercise, and dynamic arterial compliance," *Circulation* **102**(11), 1270–1275 (2000).

48. I. V. Tikhonova, A. V. Tankanag, and N. K. Chemeris, "Time-amplitude analysis of skin blood flow oscillations during the post-occlusive reactive hyperemia in human," *Skin Res. Technol.* **19**(1), e174–e181 (2013).

49. G. B. Yvonne-Tee et al., "Method optimization on the use of postocclusive hyperemia model to assess microvascular function," *Clin. Hemorheol. Micro.* **38**(2), 119–133 (2008).

50. N. R. Harris and R. E. Rumbaut, "Age-related responses of the microcirculation to ischemia-reperfusion and inflammation," *Pathophysiology* **8**(1), 1–10 (2001).

51. E. Konstantinova et al., "Plasma lipid levels, blood rheology, platelet aggregation, microcirculation state and oxygen transfer to tissues in young and middle-aged healthy people," *Clin. Hemorheol. Microcirc.* **30**(3), 443–448 (2004).

52. T. Ryan, "The ageing of the blood supply and the lymphatic drainage of the skin," *Micron* **35**, 161–171 (2004).

53. R. I. Kelly et al., "The effects of aging on the cutaneous microvasculature," *J. Am. Acad. Dermatol.* **33**(5), 749–756 (1995).

54. J. P. Noon et al., "Impaired microvascular dilatation and capillary rarefaction in young adults with a predisposition to high blood pressure," *J. Clin. Invest.* **99**(8), 1873 (1997).

55. E. Sadoun and M. Y. Reed, "Impaired angiogenesis in aging is associated with alterations in vessel density, matrix composition, inflammatory response, and growth factor expression," *J. Histochem. Cytochem.* **51**(9), 1119–1130 (2003).

56. P. E. Gates, W. D. Strain, and A. C. Shore, "Human endothelial function and microvascular ageing," *Exp. Physiol.* **94**(3), 311–316 (2009).

57. F. Bari et al., "Flow motion pattern differences in the forehead and forearm skin: age-dependent alterations are not specific for Alzheimer's disease," *Microvasc. Res.* **70**(3), 121–128 (2005).

58. W. L. Kenney and T. A. Munce, "Invited review: aging and human temperature regulation," *J. Appl. Physiol.* **95**(6), 2598–2603 (2003).
59. M. El-Domyati et al., "Intrinsic aging vs. photoaging: a comparative histopathological, immunohistochemical, and ultrastructural study of skin," *Exp. Dermatol.* **11**(5), 398–405 (2002).
60. B. A. Gilchrest, "Skin aging and photoaging: an overview," *J. Am. Acad. Dermatol.* **21**(3), 610–613 (1989).
61. J. M. Waller and H. I. Maibach, "Age and skin structure and function, a quantitative approach (i): blood flow, ph, thickness, and ultrasound echogenicity," *Skin Res. Technol.* **11**(4), 221–235 (2005).
62. S. Hagisawa, J. C. Barbenel, and R. M. Kenedi, "Influence of age on postischaemic reactive hyperaemia," *Clin. Phys. Physiol. Meas.* **12**(3), 227 (1991).
63. C. T. Minson et al., "Decreased nitric oxide-and axon reflex-mediated cutaneous vasodilation with age during local heating," *J. Appl. Physiol.* **93**(5), 1644–1649 (2002).
64. L. A. Holowatz et al., "Nitric oxide and attenuated reflex cutaneous vasodilation in aged skin," *Am. J. Physiol.* **284**(5), H1662–H1667 (2003).
65. M. A. James et al., "Effects of aging and hypertension on the microcirculation," *Hypertension* **47**(5), 968–974 (2006).
66. J. O'Doherty et al., "Comparison of instruments for investigation of microcirculatory blood flow and red blood cell concentration," *J. Biomed. Opt.* **14**(3), 034025 (2009).
67. M. A. Black, D. J. Green, and N. T. Cable, "Exercise prevents age-related decline in nitric-oxide-mediated vasodilator function in cutaneous microvessels," *J. Physiol.* **586**(14), 3511–3524 (2008).
68. G. J. Hodges et al., "Influence of age, sex, and aerobic capacity on forearm and skin blood flow and vascular conductance," *Eur. J. Appl. Physiol.* **109**(6), 1009–1015 (2010).
69. J. Zhong et al., "A mathematical analysis on the biological zero problem in laser Doppler flowmetry," *IEEE Trans. Biomed. Eng.* **45**(3), 354–364 (1998).
70. N. C. Abbot and J. S. Beck, "Biological zero in laser Doppler measurements in normal, ischaemic and inflamed human skin," *Int. J. Microcirc. Clin. Exp.* **12**(1), 89–98 (1993).
71. D. P. Kernick, J. E. Tooke, and A. C. Shore, "The biological zero signal in laser Doppler fluximetry-origins and practical implications," *Pflugers Arch.* **437**, 624–631 (1999).
72. T. Binzoni et al., "Haemodynamic responses to temperature changes of human skeletal muscle studied by laser-Doppler flowmetry," *Physiol. Meas.* **33**(7), 1181–1197 (2012).
73. R. Djaberi et al., "Non-invasive cardiac imaging techniques and vascular tools for the assessment of cardiovascular disease in type 2 diabetes mellitus," *Diabetologia* **51**(9), 1581–1593 (2008).

Adil Khalil is currently a PhD student in laboratory LARIS, University of Angers, France. His research interests include image processing, signal processing, biomedical applications, and more precisely the study of microvascular blood flow through laser speckle contrast images.

Anne Humeau-Heurtier received her PhD degree in signal and image processing. She is currently a professor in the University of Angers, France. Her research interests are mainly focused on the processing of laser Doppler flowmetry data and laser speckle contrast images.

Guillaume Mahé is a medical doctor at the University Hospital of Rennes. He obtained his PhD in 2011, and he is an assistant professor of vascular medicine at the University of Rennes. His main research activity is clinical research in the microcirculation field using laser and oximetry especially in patients with peripheral artery disease. Since his postdoctoral fellowship, he has been a research collaborator at the Mayo Clinic (Rochester, MN, USA).

Pierre Abraham is a cardiologist and a professor of physiology at the University of Angers. His current research interest focuses on vascular physiology and exercise. Many of his recent papers are on the clinical use of microvascular devices.